Comparative assessment of the spectral impact on the energy yield of high concentrator and conventional photovoltaic technology

Eduardo F. Fernández[1,2*], Alberto Soria-Moya[1], Florencia Almonacid[2] and Jorge Aguilera[2]

[1]Centro de Estudios Avanzados en Energía y Medio Ambiente (CEAEMA), University of Jaen, Jaen, Spain
[2]Grupo IDEA, University of Jaen, Jaen, Spain
Email: fenandez@ujaen.es, Tel: +34 9543213520

Abstract: Photovoltaic materials are spectrally selected and their electrical output is affected by the spectral distribution of the incident irradiance. The performance of high concentrator photovoltaic (HCPV) systems is more influenced by the spectral changes than conventional single-junction photovoltaic (PV) systems due to the use of multi-junction (MJ) solar cells and optical devices. Despite this, the detailed comparison of the spectral impact on the electrical output of HCPV and PV technology under the same atmospheric conditions has not been addressed yet. Because of this, this paper aims to compare the spectral impact on the energy yield of both type of devices at a monthly and annual time scale at several locations with disparate climate conditions. The spectral dependence of both technologies is quantified by using the spectral factor (SF) index in conjunction with the Simple Model of Atmospheric Radiative Transfer of Sunshine (SMARTS) at five locations of the Aerosol Robotic Network (AERONET) database. The present paper shows that the current HCPV systems present annual spectral losses of around 5% with respect to PV systems at representative locations.

Keywords: spectral impact, energy yield, high concentrator photovoltaics, photovoltaics

1. Introduction

From the outset, high concentrator photovoltaic (HCPV) technology has appeared as an alternative power source to produce more cost-effective electricity than conventional photovoltaic (PV) technology [1]. The use of optical devices to concentrate the light on high efficiency multi-junction (MJ) solar cells offers at the same time, high efficiencies and a reduction in the amount of semiconductor material [2]. The limit of the efficiency of MJ solar cells and HCPV systems is far from being reached, and an increase of 10% within the next decade is expected [3]. Taking this into account, the cumulative installed capacity of HCPV technology is tending to grow from a value of 358MWp at the end of 2014 to more than 1GWp in 2020 [4]. At the same time, the levelised cost of electricity (LCOE) is tending to decrease, LOCE = 0.035-0.080 €/kWh in 2020, and reach lower values than conventional PV technology at locations with high annual direct normal irradiation [5]. All the above show the great potential of this technology to play an important role in the energy generation market within next decades.

On the other hand, the maturity and understanding of HCPV technology when operating in outdoors is clearly lower than conventional PV technology. Because of this, important efforts are still needed in order to achieve a better understanding, increase the investors' confidence and therefore promote the market expansion of HCPVs as a real alternative energy source to conventional PVs [6]. One of the more relevant differential issues between HCPV and PV technology is related with the influence of the spectral variations on their electrical output [7]. The use of MJ solar cells based on the internal series connection of several subcells with different energy gaps [8], and optical devices which modify the spectral distribution that strikes on the solar cells surface [9], make HCPV devices more sensitive to the incident spectral distribution.

Because of this, the scientific community has devoted great efforts to understand the impact of the input spectrum on the performance of HCPV technology under real operating conditions. The use of the SMARTS model in conjunction with AERONET data source have been used by Muller et al. [10] to evaluate the effect of air mass, aerosol optical depth and precipitable water on the performance of different HCPV modules in Golden (USA) over 9 months. Hashimoto et al. [11] studied the impact of spectral changes on the performance of different HCPV one-cell modules during a clear and a very clear day through the SMR (spectral matching ratio) index measured with a spectroradiometer. An alternative procedure based on isotype solar cells and the spectral parameter Z has been proposed by Peharz et al. [12, 13] to evaluate the spectral impact on the electrical output of different HCPV modules over several months at Freiburg (Germany). A similar approach based on the SMR index registered with isotype solar cells has been also used by García-Domingo et al. [14] to evaluate the spectral impact on the electrical characteristics of various HCPV modules over the course of a year in Jaen (Spain). The contour diagram of the performance ratio of a HCPV system analysed during a year at Miyazaki (Japan), as a function of the cell temperature and spectrum, quantified with the APE (Average Photon Index) index gathered with a spectroradiometer, has been obtained by Husna et al. [15]. The studies above are focused on analysing the instantaneous impact of spectral variations on the performance of HCPV modules or systems. Other recent work addresses the spectral impact on an annual time scale since it is directly related with the annual energy yield of the systems. Victoria et al. [16] quantified the annual spectral losses on the energy yield of different HCPV modules in Madrid (Spain) by the use of the SMR index measured with isotype solar cells. Fernández et al. [17] evaluated the annual average spectral impact on the performance of several HCPV modules made up of different types of MJ solar cells and optical devices through the spectral factor (SF) index with spectra simulated with the SMARTS model and data obtained from AERONET at five locations (Solar Village (Saudi Arabia), Alta Floresta (Brazil), Frenchman Flat (USA), Granada (Spain) and Beijing (China)). The same HCPV modules and a similar approach have also been used by Soria-Moya et al. [18] to estimate the annual energy spectral losses as a function of latitude. Chan et al. [19] quantified the impact of air mass, aerosol optical depth and precipitable water on the annual energy harvested by a HCPV module at five AERONET sites (Rogers Dry Lake (USA), Tamanrasset (Algeria), Sede Boqer (Israel), Solar Village (Saudi Arabia) and Jaipur (India)) by using the Syracuse simulation model [20] and spectra generated with the SMARTS model.

At the same time, single-junction PV devices are also spectrally selected and their power and energy output is also affected by spectral variation under real operating conditions. Because of this, the spectral dependence of these devices is also continuously being analysed by the scientific community and a wide number of studies can be found in the literature. Minemoto et al. [21] analysed the impact of the spectral variations in some PV devices as a function of the APE index measured with a spectroradiometer, as well as the contour diagrams of the performance ratio of several PV devices as a function of APE and module temperature [22, 23, 24, 25], over the course of a year at Kusatsu (Japan).

The APE and SF indexes gathered with a spectroradiometer have been used by Ishii et al. [26] to evaluate the spectral impact on the performance ratio of a wide number of PV technologies during 17 months at eight selected locations in Japan (Sapporo, Nakatsugawa, Otsu, Kobe , Katsuragi, Tosu, Isahaya and Okinoerabu). A similar approach has been followed by Nofuentes et al. [27] to analyse the spectral dependencies of some commercial PV devices during a year at Jaen (Spain). The work above represent examples of studies concerning the instantaneous impact of spectral changes on the performance of PV devices. As in the case of HCPV technology, other researchers have recently conducted different studies to analyse the spectral impact on an annual or monthly time scale. Abella et al. [28] quantified the spectral impact on the monthly and annual energy yield of a wide number of commercial PV devices by using the SEDES2 spectral model and Meteonorm software at four locations (Stuttgart (Germany), Tamanrasset (Algeria), Madrid (Spain) and Jaen (Spain)). Fernández et al. [29, 30] evaluated the average annual spectral impact on the performance of various new generation solar cells by also using the SF index in conjunction with the SMARTS model at six AERONET locations (Solar Village (Saudi Arabia), Alta Floresta (Brazil), Frenchman Flat (USA), Granada (Spain), Beijing (China) and Edinburgh (Scotland)). The analysis of the effect of spectral variations on the monthly and annual energy yield of different commercial PV devices, by using the SF index and spectral measurements of around 3.5 years performed with a spectroradiometer, has been also conducted by Dirnberger et al. [31] at Freiburg (Germany).

The examples above represent relevant studies concerning the analysis of the effect of spectral variations on the performance of both technologies. These studies allow different conclusions to be reached. It seems clear that HCPV systems show a higher spectral dependence than conventional PV systems. However, it can be also concluded that the impact of the spectral variations on both technologies depends on the atmospheric characteristics of each particular site (i.e. air mass, aerosol optical depth and precipitable water). Moreover, the procedures and approaches used by the authors to analyse the spectral impact on HCPV and PV technology are different. Hence, based on the current studies, the direct comparison between the spectral impact on the electrical output of HCPV and PV technology under the same climate conditions is not possible and has not been done At the same time, the energy harvested by photovoltaic systems is directly related with their bankability [32]. Bearing this in mind, this paper is focused on the comparative evaluation of the spectral impact on the energy yield of HCPV and PV technologies under a wide range of atmospheric conditions. In order to achieve this goal, the approach previously used by the authors in [17], where the annual average spectral impact on the performance of several HCPV systems but not on the energy yield was analysed, has been followed. So, the present study allows the analysis and comparison between the performance and potential of HCPV and PV technologies to be done in terms of the spectral behaviour.

2. Methods and materials

2.1. Spectral factor and energy yield

The power output of a HCPV or PV system is mainly determined by the incident irradiance, spectral distribution and the operating cell temperature. Hence, the maximum power (P) of a PV device can be expressed with a low margin of error as [26]:

$$P \approx \frac{P^*}{G^*} \cdot G \cdot TF \cdot SF \tag{1}$$

and of a HCPV device as [33]:

$$P \approx \frac{P^*}{DNI^*} \cdot DNI \cdot TF \cdot SF \tag{2}$$

where P^*, G^* and DNI^* are the maximum power, global irradiance and direct normal under the standard test conditions (STC), G and DNI are the incident global and direct normal irradiance, TF is the thermal factor and SF is the spectral factor.

The TF quantifies the effect of cell temperature of the power output of a PV and HCPV device as [27, 34]:

$$TF = 1 + \gamma(T_c - T_c^*) \tag{3}$$

where γ is the maximum power temperature coefficient, T_c is the cell temperature and T_c^* is the cell temperature under STC.

The spectral factor quantifies the influence of the input spectrum on the power output of a single-junction PV device as [35]:

$$SF = \frac{\int E_g(\lambda)SR(\lambda)d\lambda \int E_{g,ref}(\lambda)d\lambda}{\int E_{g,ref}(\lambda)SR(\lambda)d\lambda \int E_g(\lambda)d\lambda} \tag{4}$$

where λ is the wavelength, $E_g(\lambda)$ is the incident global spectral distribution, $E_{g,ref}(\lambda)$ is the reference global spectrum and $SR(\lambda)$ is the spectral response of the PV device.

Following the same approach, the impact of the incident spectral distribution on the power output of a HCPV device can be expressed as [17]:

$$SF = \frac{\min(\int E_b(\lambda)\eta(\lambda)SR_i(\lambda)d\lambda) \int E_{b,ref}(\lambda)d\lambda}{min(\int E_{b,ref}(\lambda)\eta(\lambda)SR_i(\lambda)d\lambda) \int E_b(\lambda)d\lambda} \tag{5}$$

where the *i*-index represents the junction of the MJ solar cell, $E_b(\lambda)$ is the incident direct normal spectral distribution, $E_{b,ref}(\lambda)$ is the direct reference spectrum and $\eta(\lambda)$ is the spectral optical efficiency.

The SF quantifies the instantaneous spectral impact as the ratio of the short-current density at operating conditions relative to the short-current density under STC: an SF higher than 1 indicates spectral gains while an SF lower than 1 indicates spectral losses. This index has been experimentally demonstrated to be valid to approximate the spectral gains or losses on the power output of HCPV and conventional single-junction PV devices [33, 36, 37], and therefore allows the direct comparison of the spectral impact on the maximum power of HCPV and PV devices to be done.

The energy harvested by a PV or HCPV system during a specific period of time T can be estimated from equations (1) and (2) as:

$$E \approx \int_T \; P(I, T_c, E(\lambda))dT = \frac{P^*}{I^*} \cdot \int_T \; I \cdot TF(T_c) \cdot SF(E(\lambda))dt \tag{6}$$

where I represents the incident irradiance: I = G for a PV system and I = DNI for a HCPV system, and $E(\lambda)$ represent the incident spectral distribution: $E(\lambda) = E_g(\lambda)$ for a PV system and $E(\lambda) = E_b(\lambda)$ for a HCPV system.

Since the aim is the individual estimation of the spectral impact on the energy produced, the thermal effects have to be neglected in equation (6) (TF = 1). So, the relative spectral impact on the energy yield for a desired period of time can be expressed as:

$$\Delta E(\%) \approx 100 \cdot \left(\frac{\frac{P^*}{I^*}\cdot\int_T I\cdot SF\big(E(\lambda)\big)dt - \frac{P^*}{I^*}\cdot\int_T I\cdot SF\big(E_{ref}(\lambda)\big)dt}{\frac{P^*}{I^*}\cdot\int_T I\cdot SF\big(E_{ref}(\lambda)\big)dt}\right) \quad (7)$$

since $SF(E_{ref}(\lambda)) = 1$, equation (7) becomes:

$$\Delta E(\%) \approx 100 \cdot \left(\frac{\int_T I\cdot SF\big(E(\lambda)\big)dt - \int_T Idt}{\int_T Idt}\right) = 100 \cdot \left(\frac{\int_T I\cdot SF\big(E(\lambda)\big)dt}{\int_T Idt} - 1\right) \quad (8)$$

and in normalized form as:

$$\Delta E \approx \frac{\int_T I\cdot SF\big(E(\lambda)\big)dt}{\int_T Idt} \quad (9)$$

The reasoning above that leads to equations (8) and (9) is essentially the same as the procedures discussed in [28, 31] and the one based on component cells presented in [38].

2.2. Materials

To conduct this study, four HCPV and five PV typical devices have been considered. Two of the HCPV systems are based on lattice-matched (LM) triple-junction gallium indium phosphide (GaInP)/gallium indium arsenide (GaInAs)/germanium (Ge) solar cells and the other two are based on metamorphic-mismatched (MM) triple-junction gallium indium phosphide (GaInP)/gallium indium arsenide (GaInAs)/germanium (Ge) solar cells. One of the systems formed by LM/MM monolithic triple-junction solar cells uses Fresnel lenses based on poly(methylmethacrylate) (PMMA) material and the other uses Fresnel lenses based on silicon on glass (SOG) material as primary optics to concentrate the light around 700x. Figure 1 shows the spectral response of the cells and transmittance of the Fresnel lenses considered and table 1 shows the average transmittance of the four systems in the spectral absorption band of each junction of the LM and MM cells. The five PV technologies consist of monocrystalline silicon (m-Si), polycrystalline silicon (p-Si), amorphous silicon (a-Si), cadmium telluride (CdTe) and copper indium gallium selenide (CIGS). The spectral response of each of these materials is shown in figure 2. The data of the PV materials have been taken from [28, 31], while further information of the HCPV systems considered can be found in [17]. The technologies above have been selected because they cover virtually all the photovoltaic market share. So, the results of this work could be considered representative of the current HCPV and PV systems.

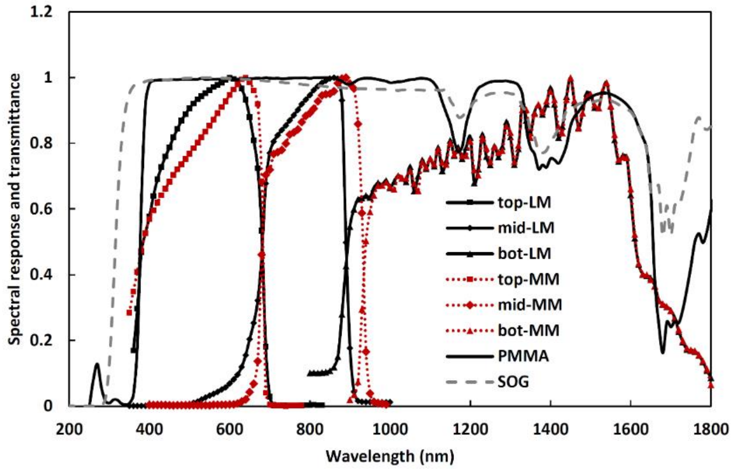

Figure 1. Normalised spectral response of the lattice-matched and metamorphic-mismatched solar cells, and transmittance of the Fresnel lenses (PMMA and SOG) used for estimating the spectral factor.

		Average transmittance (%)		
Cell	**Lens**	**Top**	**Middle**	**Bottom**
LM	PMMA	73	92	74
	SOG	87	91	82
MM	PMMA	73	92	76
	SOG	87	90	81

Table 1. Average transmittance of Fresnel lenses in the spectral band of each subcell of the lattice-matched and the metamorphic-mismatched multi-junction solar cells of the HCPV systems considered.

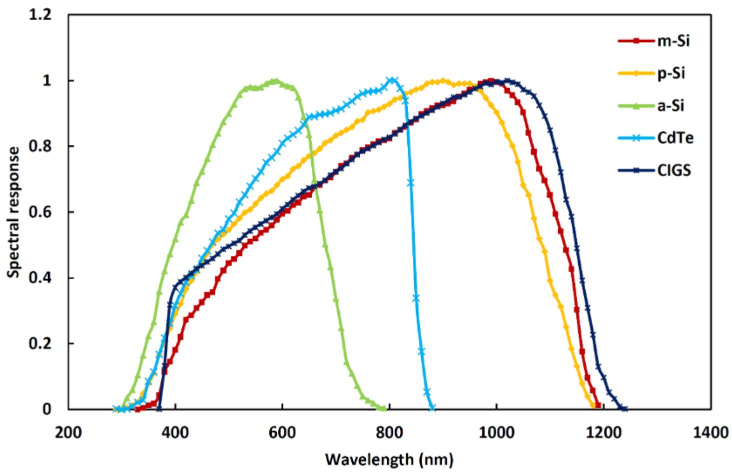

Figure 2. Normalised spectral response of different single-junction photovoltaics materials used for estimating the spectral factor.

3. Instantaneous impact of atmospheric parameters

The electrical output of HCPV or PV devices is affected by the variations of the incident spectral distribution. The air mass, aerosol optical depth (usually evaluated at 500 or 550nm) and precipitable water have been demonstrated to be the relevant atmospheric parameters to accurately evaluate the spectral impact on the electrical characteristics of photovoltaic devices [7, 19, 35]. The variation of air mass (AM) during the course of a day has a strong impact in the incoming spectral irradiance because of scattering and absorption phenomena. AM can be defined as the relation between the optical path length of the solar beam through the atmosphere and the optical path through a standard atmosphere at sea level with the sun at the zenith. This factor can be approximated to a pure geometrical parameter function of the solar position whose minimum and maximum values are 1 (a solar zenith angle of 0^o) and 38 (a solar zenith angle of 90^o) [39]. Aerosols are small particles suspended in the air either in solid or liquid state that scatter and absorb sunlight, and aerosol optical depth (AOD) is the physical magnitude to quantify their influence in the solar irradiance. The influence of aerosols in the spectral irradiance can be approximated by the Ångström turbidity formula as $AOD = AOD_{550}(\lambda/0.55)^{-\alpha}$. In this equation, AOD_{550} is the amount of aerosols in a vertical column of the atmosphere at 550nm, λ is the wavelength and α is the Ångström or wavelength exponent [40]. The presence of water vapour in the atmosphere has an important absorption effect on the incident spectral distribution. Although there are several ways to quantify the water vapour content, the widely used way to evaluate this quantity is through the precipitable water (PW). PW corresponds to the volume of liquid water that would be obtained if all the water vapour aloft were condensed [41].

The influence of AM, AOD_{550} and PW in both the global and direct normal irradiance is plotted in figure 3. As can be seen, the higher the atmospheric parameter the higher the attenuation and therefore the lower the irradiance. However, the effect of each atmospheric parameter also has a strong impact on the spectral distribution. Regarding AM, the attenuation is larger in the UV region of the spectrum, so that the increase of AM results in a progressive red shift of the spectral distribution. Regarding AOD_{550}, the attenuation is also larger at the shorter wavelengths of the spectrum and also produces a red shift of the spectrum. However, in this case that largest attenuation is located in the UV-visible part of the spectrum. Finally, PW produces a clear larger attenuation in the near-infrared part of the spectral distribution. Based on the above, it is obvious to see that the variations of each atmospheric parameter above will produce different effects on the performance of the photovoltaic materials shown in figures 1 and 2 since their absorption bands are located in different parts of the spectrum. Moreover, the effect of the variations of each atmospheric parameter affects the global and direct components of the irradiance to a different extent. This can be clearly seen in figure 3 (middle) where the attenuation of the direct component of the irradiance is around 3 times higher than in the global component by increasing the value of AOD_{550} from 0.2 to 0.8. Taking this into account, the different impact of spectral variations in HCPV and PV devices will be due to their different abortion bands but also to the different effect of each specific atmospheric parameter in each component of the radiation. To understand this issue better, an individualized analysis of the impact of each atmospheric parameter on the performance of HCPV and PV technologies is conducted. To achieve this goal, several spectra are simulated with the Simple Model of the Atmospheric Radiative Transfer of Sunshine (SMARTS) [42]. These spectra are generated varying one of the atmospheric parameters while the rest are kept constant at the reference values defined by the AM1.5G ASTMG-173-03 reference spectrum [43]. The values of AM, AOD_{550} and PW are varied from a low to an extreme value as observed in more than 350 worldwide sites of the Aerosol Robotic Network (AERONET) database [44]. The instantaneous impact of each generated spectrum is estimated by solving the SF index as defined in equations (4) and (5) and the data shown in figures 1 and 2. This allows the performance of HCPV and PV under study to be understood and compared in a wide range of real operating conditions. It should be highlighted that the results regarding the HCPV systems have already been presented in [17]. However, they are also shown below in order to better understand the differential performance between HCPV and PV technologies under the changes of the main atmospheric variables.

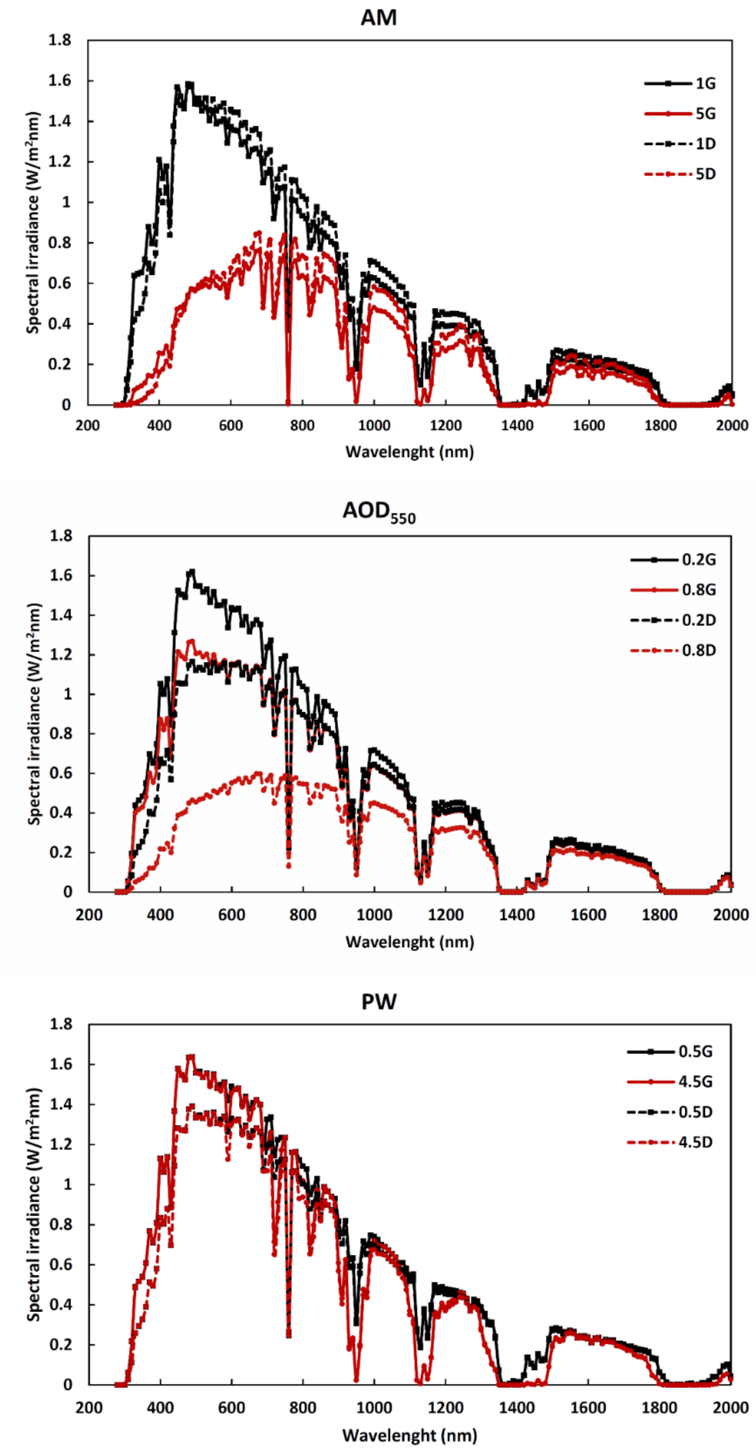

Figure 3. Impact on the global (denoted as G) and direct (denoted as D) spectral irradiance of air mass (top), aerosol optical depth at 550nm (middle) and precipitable water (bottom) simulated with the SMARTS model. The other parameters are kept constant at the reference values defined by the AM1.5d ASTMG-173-03 reference spectrum.

3.1. Impact of air mass

Figure 4 shows the spectral impact of AM variations on the performance of the HCPV (top) and PV (bottom) devices considered. As can be seen, the impact of AM is clearly higher in the performance of the HCPV systems. The four systems show a similar behaviour under AM variations. They have a maximum where the top and middle junctions generate the same current (current-matched condition) that leads to feeble spectral gains for both systems based on SOG lenses. On the left of this maximum, the performance of the HCPV systems decreases by the current limitation of the middle junction until a value around -3.5%, while on the right side it decreases by the current limitation of the top junction until values around -45% and -50%. It is also worth mentioning that the LM + PMMA and MM + SOG devices show the worst and best performance respectively. This can be explained due to the fact that the SOG Fresnel lens has a higher transmittance in the spectral region of the top junction and due to the red shift of the absorption bands of the top and middle junctions of the MM solar cell. This analysis also indicates that spectral losses under real operating conditions of the HCPV devices will be dominated by the limitation of the current of the top junction that can be explained by its higher energy gap. Among the PV devices, the a-Si and CdTe PV materials also present a notable spectral dependence under AM variations since their absorption bands are mainly located in the blue part of the spectrum. Both materials have a similar behaviour and show slight spectral gains for low AM values and significantly spectral losses as AM increases with a maximum around -40% (a-Si) and -14% (CdTe). The worse performance of the a-Si compared with the CdTe material can be explained due to its wider ban gap. The other PV materials show a stable and similar performance under AM variations. As can be seen, these materials have slight spectral losses for low AM values and spectral gains as AM increases with a maximum around 7.5% (m-Si), 3.9% (p-Si) and 5.4% (CIGS). This behaviour can be explained due to their low energy gap and wide absorption band located not only in the blue part of the spectral irradiance.

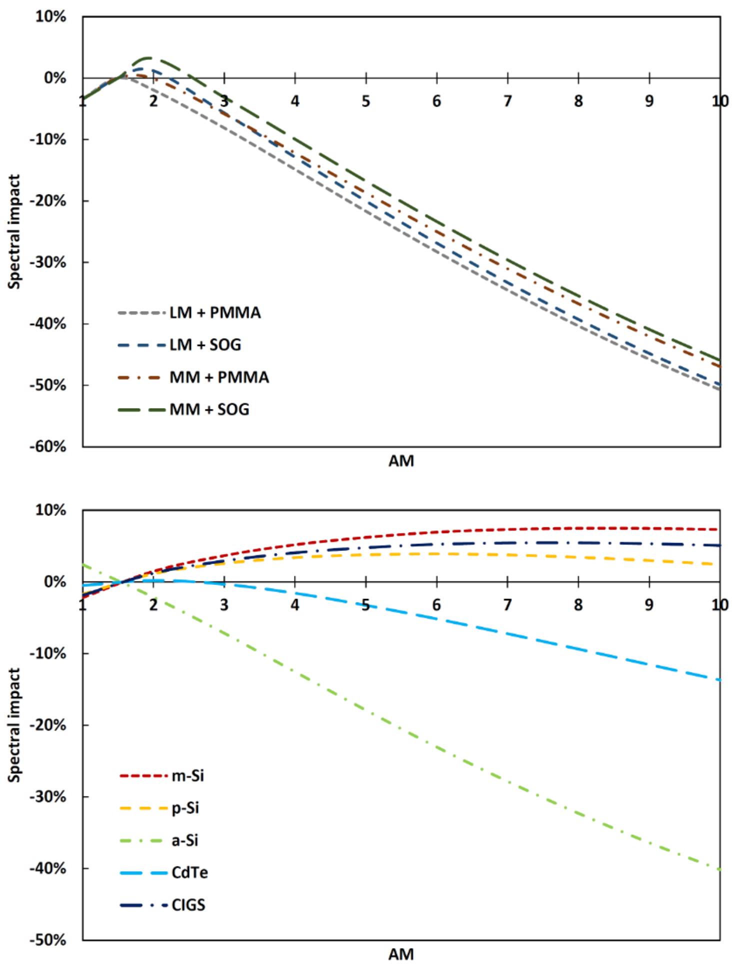

Figure 4. Individual impact of air mass on the performance of the HCPV (top) and PV (bottom) technologies under study. The other parameters are kept constant at the reference values defined by the AM1.5d ASTMG-173-03 reference spectrum.

3.2. Impact of aerosol optical depth

Figure 5 shows the spectral impact of AOD_{550} variations on the performance of the HCPV (top) and PV (bottom) devices considered. As in the previous case, the impact of AOD_{550} is similar and higher in the performance of the HCPV systems. The systems have a maximum at current-matched condition where the systems based on SOG lenses also present slightly spectral gains. On the left of this maxima, the middle junction is limiting the current, and on the right side the top junction is limiting the current decreasing the performance of the HCPV systems until values around -30% and -35%. Again, the LM + PMMA and MM + SOG systems show the worst and best performance respectively for the same reason mentioned in the previous section. As in the previous case, the a-Si and CdTe devices present the highest spectral dependence under AOD_{550} variations among all the PV materials. Both show slightly spectral gains for low AOD_{550} values and significantly spectral losses for high AOD_{550} values with a maximum around -7% (a-Si) and -4% (CdTe). The worse performance of the a-Si is also explained by its higher energy gap. It is important to highlight that the spectral losses produced in these two devices by the increase of AOD_{550} are significantly lower than by the increase of AM due to the lower impact of aerosols in the global irradiance. The other PV materials show a small influence under AOD_{550} variations due to the low effect of aerosols in the global irradiance and to their narrow ban gap. The three materials have slightly spectral gains for low AOD_{550} values and spectral losses as this factor increases with a maximum around -1%.

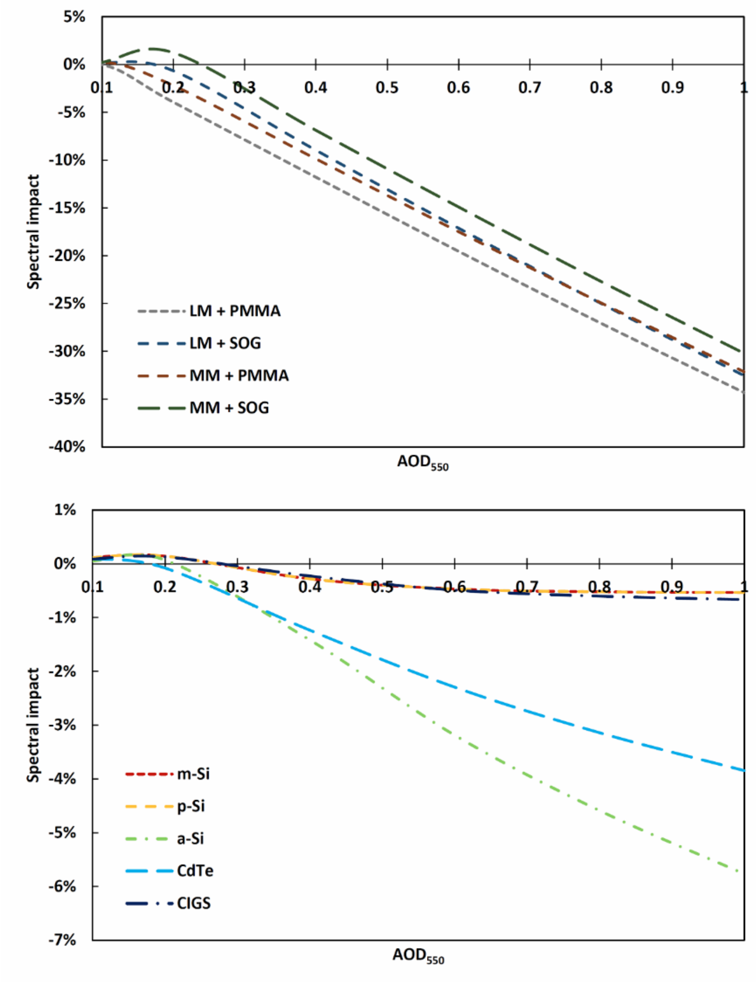

Figure 5. Individual impact of aerosol optical depth on the performance of the HCPV (top) and PV (bottom) technologies under study. The other parameters are kept constant at the reference values defined by the AM1.5d ASTMG-173-03 reference spectrum.

3.3. Impact of precipitable water

Figure 6 shows the spectral impact of PW variations on the performance of the HCPV (top) and PV (bottom) devices considered. In this case, the HCPV and PV materials show a similar performance. The HCPV systems based on LM solar cells and the a-Si and CdTe PV devices present spectral losses for low PW values and spectral gains as this parameter increases. This can be explained since the increase of PW mainly decreases the spectral irradiance in the near-infrared region. As a result, the current of the top and middle junctions of the LM solar cells and the a-Si and CdTe materials keep almost constant resulting in an overall increase of the performance of the materials with PW. The top and middle junctions of the MM solar cell and the m-Si, p-Si and CIGS materials can absorb lower energetic photons in the near-infrared region. Because of this, although these materials also show spectral losses for low PW values, the ratio between the effect of PW on the irradiance and the current of these devices keeps almost constant resulting in a more stable performance under PW variations.

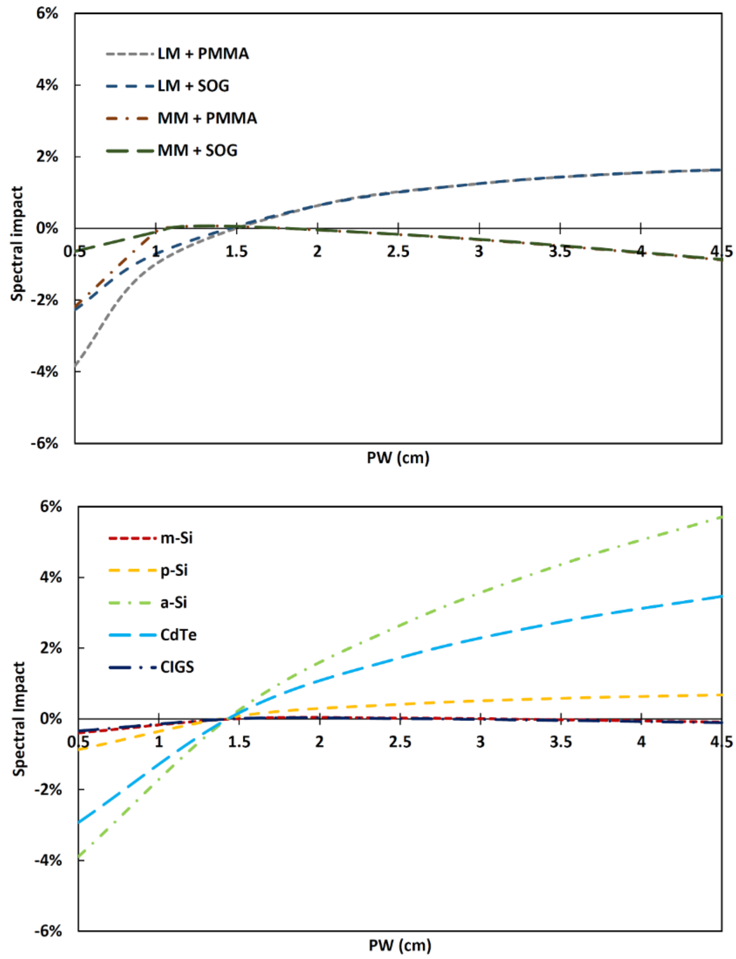

Figure 6. Individual impact of aerosol optical depth on the performance of the HCPV (top) and PV (bottom) technologies under study. The other parameters are kept constant at the reference values defined by the AM1.5d ASTMG-173-03 reference spectrum.

From the analysis above it can be concluded that the HCPV systems have a larger spectral sensitivity than the PV devices under spectral variations. Moreover, the air mass has been demonstrated to be the atmospheric parameter with the largest impact on the performance of both the HCPV and PV devices. This suggests that the effects of the spectral variations on the energy yield of both technologies under real operating conditions are going to be mainly dominated by this factor. The aerosol optical depth has been also found to produce a strong impact on the performance of the HCPV systems but not as high on the PV materials. This is due to the different absorption bands of the materials but also to the significantly lower effect of the aerosol optical depth in the global than in the direct component of the radiation. At the same time, the third parameter with the largest impact on the performance of the HCPV systems is PW, but this leads to similar effects to the aerosol optical depth in the PV devices. Moreover, contrary to the other two atmospheric parameters, PW produces a similar impact on the performance of both technologies. This can be mainly explained since PW produces almost equal effects in the global and direct irradiance due to the fact that it mainly absorbs but does not scatter the incoming irradiance. So, contrary to AM and AOD, the presence of PW in the atmosphere does not produce diffuse irradiance that contribute to the global component of the radiation. The results above indicate that the spectral effects in the performance of HCPV and PV materials will be different and determined by the absorption band of each specific device. However, the different influence of each atmospheric parameter in the amount and spectral distribution of the global and direct irradiance is also a key parameter that needs to be considered.

4. Spectral impact on the energy yield

In the last section, the analysis and comparison of the instantaneous impact of each individual atmospheric parameters on the performance of HCPV and PV devices was undertaken. This is useful to achieve a better understanding of the behaviour of both technologies. However, to properly compare the spectral impact on the energy yield of both technologies, is necessary to take into account the effect of all the time-varying atmospheric parameters on the amount and spectral distribution of the irradiance for the desired period of time. In this section, the spectral influence on the energy yield of both technologies at selected locations with disparate climate conditions is conducted. First of all, the chosen sites together with their atmospheric characteristics are listed, as well as the procedure followed to simulate the time-series of the spectral distribution. After that, the analysis of the spectral impact on the energy harvested of all photovoltaic technologies considered at a monthly and annual time scale is conducted.

4.1. Locations and spectra simulation

The following five sites have been selected:

- Solar Village (Saudi Arabia): lat. N 24º54'25'', long. E 46º23'49''
- Alta Floresta (Brazil): lat. S 09º52'15'', long. W 56º06'14''
- Frenchman Flat (USA): lat. N 36º48''32'', long. W 115º56'06''
- Granada (Spain): lat. N 37º09'50'', long. W 03º36'18''
- Beijing (China):lat. N 39º58'37'', long. E 116º22'51''

These locations have been chosen since they represent places with diverse climate conditions over different continents and latitudes. So, it allows the performance of HCPV and PV systems to be studied and compared in a wide range of real operating conditions. Moreover, the atmospheric parameters of these locations can be obtained from the AERONET database. The AERONET program is a federation of ground-based sun photometer sensors established by NASA and PHOTONS which started in the early 1990s [45]. It offers measurements of aerosol optical depth and other relevant atmospheric parameters at remote sites for three data quality levels (i.e. Level 1, Level 1.5 and Level 2). Hence, high-quality observed values of the relevant atmospheric parameters for these sites were available to accurately estimate the incident spectra. Figure 7 shows the monthly-average values of the atmospheric parameters gathered from AERONET in order to show the atmospheric characteristics of the locations considered. Solar Village is a desert location with medium values of precipitable water and high values of aerosol optical depth dominated by dust emissions. Alta Floresta is a tropical site with the typical high values of precipitable water of these locations, and high values of aerosol optical depth from August to October produced by biomass burning in the

Amazon. Frenchman Flat is a clay desert location with medium values of precipitable water and is characterized by a clear atmosphere with very low values of aerosol optical depth. Granada is a non-industrialized medium city with medium values of precipitable water and aerosol optical depth periodically affected by Saharan dust. Finally, Beijing is an industrialized city with medium values of precipitable water and is characterized by a highly polluted atmosphere with extreme values of aerosol optical depth. Further information about the climatology of these sites can be found for instance in [46, 47, 48, 49], as well as at AERONET website.

In order to estimate the spectral impact on the energy yield of each material is necessary to know the spectral distribution of the irradiance at every instant of time. To conduct this, AM was calculated as a function of Sun´s zenith angle (θ) every ten minutes as [50]:

$$AM = \frac{1}{cos\theta + 0.45665\theta^{0.07}(96.4836-\theta)^{-1.697}} \quad (10)$$

and the daily values of AOD_{550}, α and PW were obtained from the AERONET database [51], while the rest of input parameters of the SMARTS model were kept constant at the reference values (AM1.5G ASTMG-173-03 spectrum). Table 2 shows the number and quality of available data at each specific location. Once the parameters above were available, the daily time-series of the direct and global component of the spectral irradiance for the whole year were simulated with the SMARTS model. Finally, the spectral impact on the energy yield for a desired period of time of each material has been calculated using equations (4), (5) and (9), and the data shown in figures 1 and 2. The use of high-quality observed data from AERONET in conjunction with the SMARTS model is widely used by the scientific community to evaluate the spectral performance of PV devices, as shown in the different references listed in the introduction. In addition, the analytical expressions discussed in section 2 and the procedure followed in this work to evaluate the spectral impact on the electrical output of solar devices have been previously validated by the authors in [33, 52]. In order to have a sense of the accuracy of the methodology used here, appendix I has been also included to compare the simulated results with long-term experimental data.

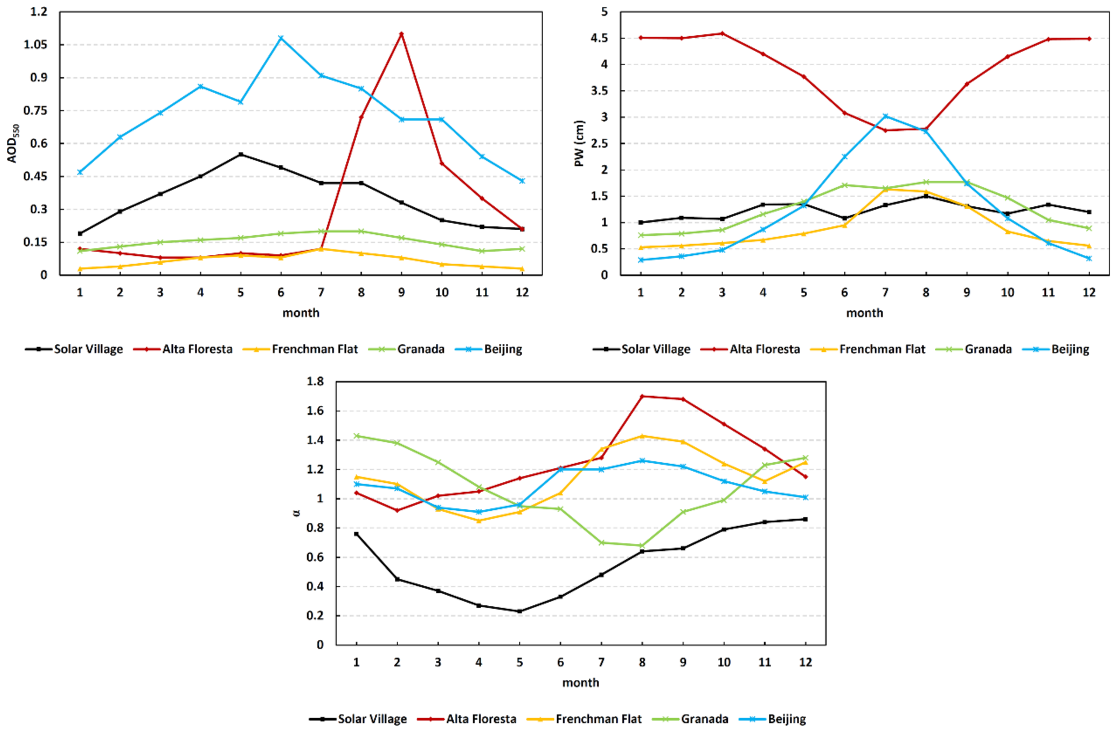

Figure 7. Monthly-average values of aerosol optical depth at 550nm (AOD_{550}), Ångström exponent (α) and precipitable water (PW) obtained from AERONET for the five sites considered.

Location	Available time period (days)	Data quality
Solar Village	3909	Level 2.0 Quality Assured Data (Highest)
Alta Floresta	3045	
Frenchman Flat	1752	
Granada	1707	
Beijing	2959	

Table 2. Number of days and quality of observed data available at AERONET database at each location considered.

4.2. Monthly impact

Figures 8 and 9 show the monthly spectral impact on the energy yield of the selected HCPV systems and PV devices for the five sites considered. As was expected from the previous study, the energy yield of the HCPV systems shows a higher monthly spectral dependence than the PV devices. Moreover, the HCPV systems have the same monthly behaviour at each particular site. Among them, the system made up of LM + PMMA and MM + SOG show the worst and best performance respectively, while the other two present similar spectral dependences. This is valid at all sites except in Alta Floresta. This site has extremely high values of PW that increase the performance of the systems based on LM solar cells as previously discussed. Taking this into account, and the extreme AOD_{550} values reached from August to October, this place shows the highest monthly variations among the five sites. The maximum difference at this location is produced by the LM + PMMA system with spectral losses ranging from -0.6% to -33.5%, and the minimum by the MM + SOG system with values ranging from -1.4% to -29.2%. The lowest monthly variations are found in Solar Village, where the maximum difference is produced by the LM + PMMA system with spectral losses ranging from -4.2% to -9.1%, and the minimum by the MM + SOG system with values ranging from -2.9% to -4.7%.

With regards to the PV materials, the a-Si and CdTe show a similar and clear higher monthly spectral dependence than the others that can be explained by their wider ban gap. The a-Si material shows the highest monthly variations in Alta Floresta, as in the case of HCPV systems, with values ranging from 8.6% to -5.6%. This strong variation is also produced by the high values of PW during all the year and by the extreme values of AOD_{550} from August to October. The CdTe material shows the highest monthly variations in Beijing with spectral losses ranging from -1.8% to -8.5%.The lowest monthly variations for both materials are produced in Solar Village with values ranging from 1.3% to -0.9% for the a-Si and values ranging from -0.6% to -1.5% for the CdTe material. The other PV materials have a stable performance and almost the same monthly variations. The highest and lowest monthly spectral variations are found for the p-Si material in Beijing and Alta Floresta with energy losses ranging from -0.5% to -3% and 0.1% to -0.3%, respectively.

Finally, it can be concluded that all the photovoltaic devices tend to have a seasonal dependence. However, this seasonal variation cannot be explained only taking into account the variation of the Sun´s position during the year, and therefore the AM variations (the parameter with the largest impact). This means that it is necessary to take into account the impact of the other atmospheric parameters to properly understand the impact of the spectrum on the energy yield of photovoltaics material. A good example of this is the strong variation produced in September in Alta Floresta for both the HCPV and PV devices due to the high AOD_{550} values produced by biomass burning in the Amazon

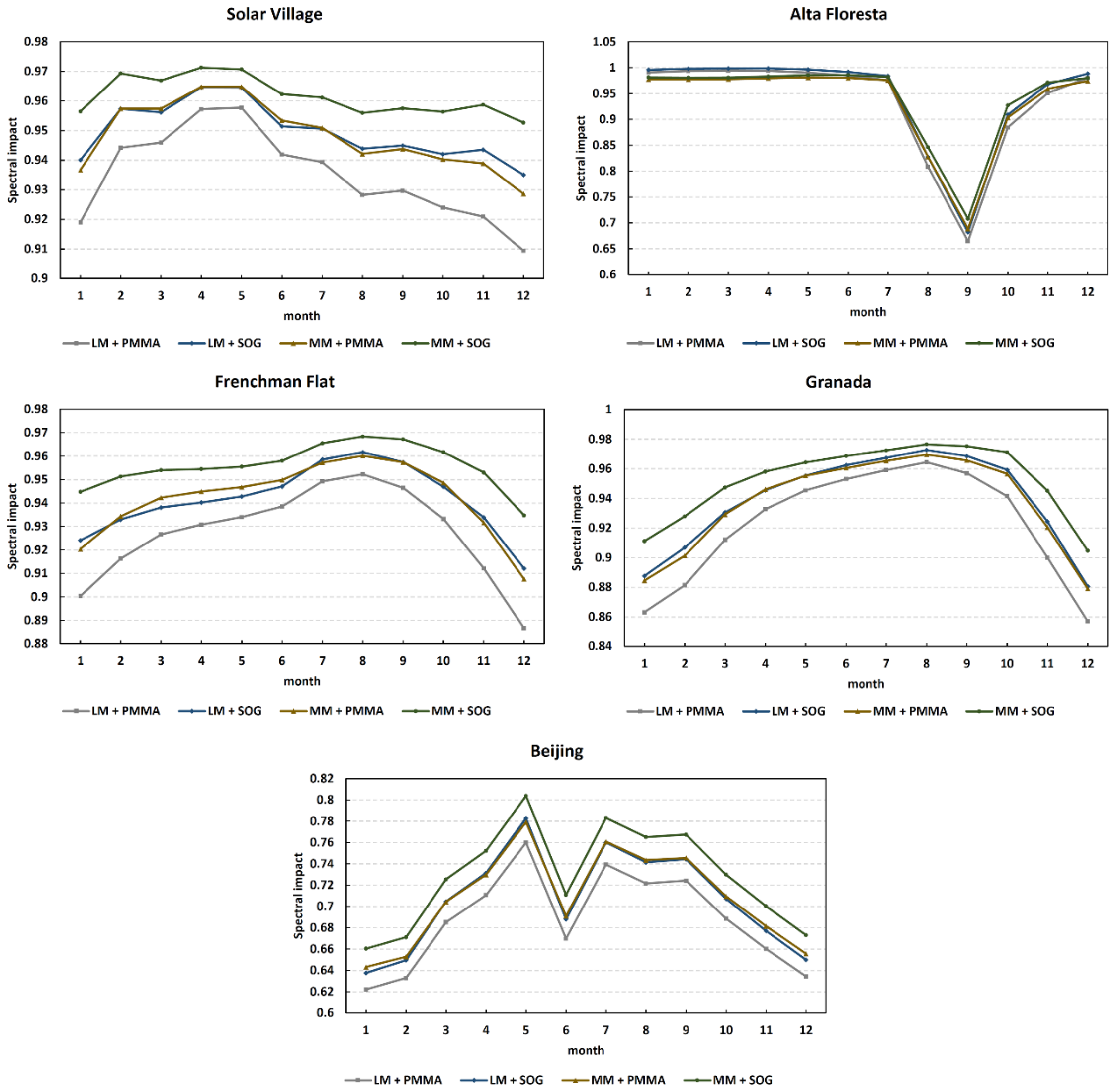

Figure 8. Impact of the spectral variation on the monthly energy yield of the HCPV materials under study for the five sites considered.

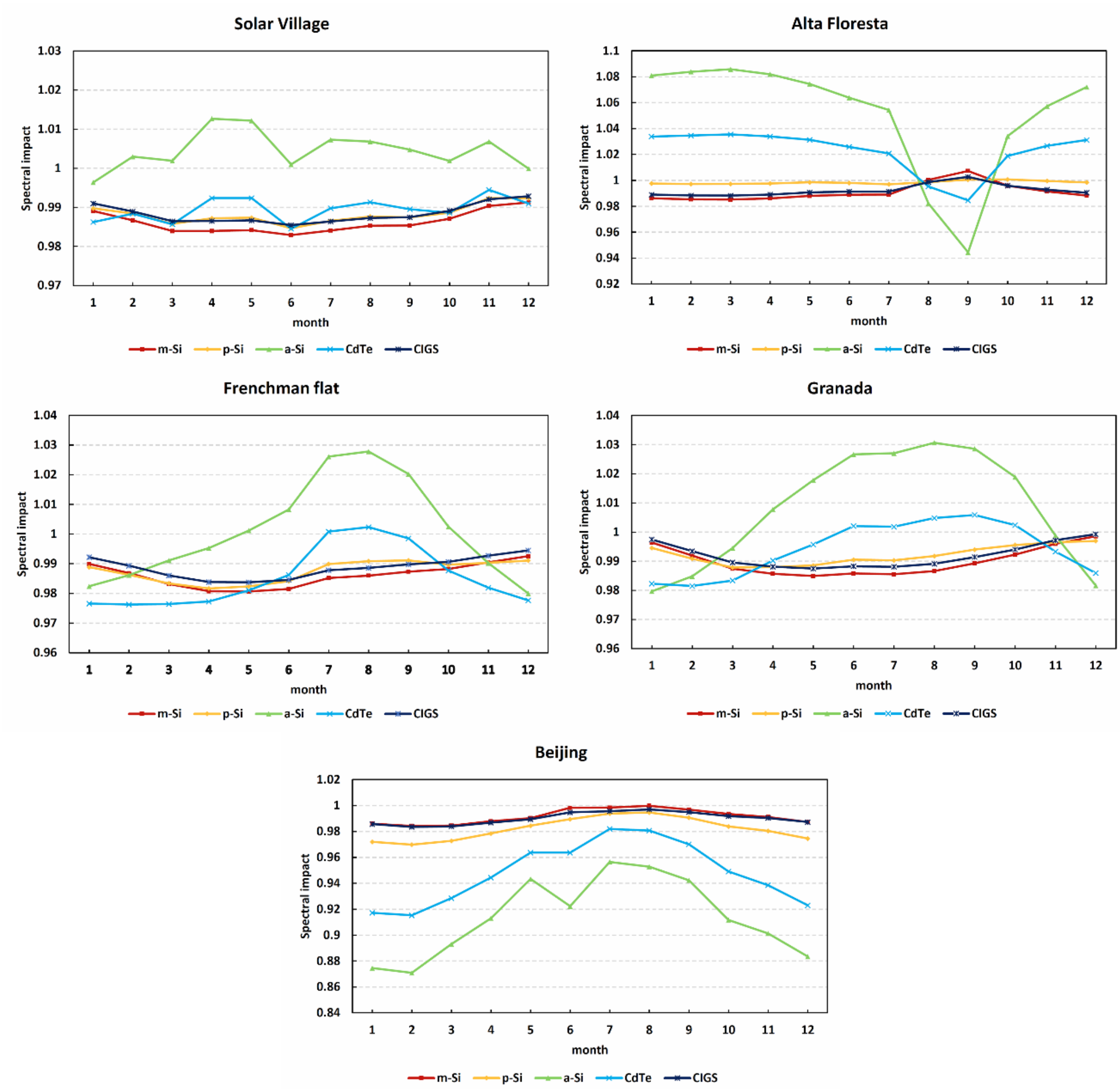

Figure 9. Impact of the spectral variation on the monthly energy yield of the PV materials under study for the five sites considered.

4.3. Annual impact

Figures 10 and 11 show the annual spectral impact on the energy yield of the HCPV and PV devices for all sites studied. As was expected, the energy yield of the HCPV systems shows a higher annual spectral dependence than the PV devices. Furthermore, the HCPV systems present relevant spectral losses and have a similar behaviour at each location. The minimum spectral losses are produced at Alta Floresta since it has the lowest AM (lowest latitude) and highest PW values, with energy losses ranging from -3.9% to -5.2%. The maximum spectral losses are produced at Beijing since it has the highest AM (highest latitude) and AOD_{550} values, with energy losses ranging from -26.5% to -30.6%. As in the monthly analysis, the LM + PMMA and MM + SOG systems have the worst and best performance and the others present similar spectral dependences, expect in Alta Floresta. Although this location has extreme AOD_{550} values from August to October, the high values of PW during all the year yield to a better performance of the systems based on LM solar cells. Among the PV materials, the a-Si and CdTe devices show the largest spectral dependence, due to their higher energy gap, and a similar behaviour for each location. As for the HCPV systems, the best and worst performance of these two materials are found in Alta Floresta and Beijing. Alta Floresta presents spectral gains of 5.4% for the a-Si device and 2.4% for the CdTe device since this location has the lowest and highest AM and PW values. Beijing presents spectral losses of -7.8% for the a-Si device and -4.6% for the CdTe device since this location has the highest AM and AOD_{550} values. As expected, the other PV materials show a stable behaviour for all locations, due to their narrow band gap, and almost the same annual energy losses. The worst and best performance is found for the p-Si materials in Beijing and Alta Floresta with energy losses of -1.6% and -0.2%.

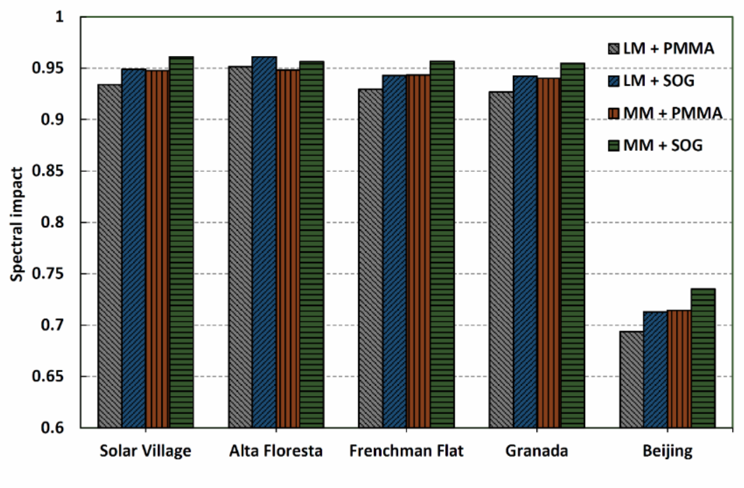

Figure 10. Impact of the spectral variation on the annual energy yield of the HCPV materials under study for the five sites considered.

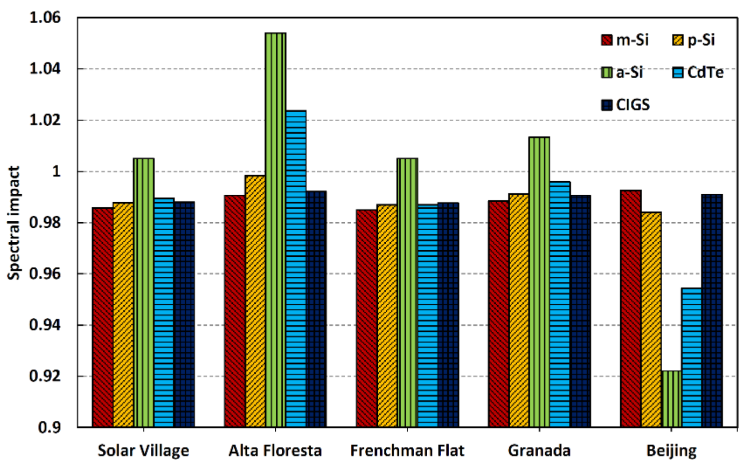

Figure 11. Impact of the spectral variation on the annual energy yield of the PV materials under study for the five sites considered.

As a summary, table 3 listed the annual maximum, minimum and average differences found between the annual spectral impact on the energy yield of the HCPV and the PV technologies. In addition, the annual differences between the spectral impact of each HCPV system and the PV materials at all the locations are shown in the appendix II (tables AII.1 to AII.4). It is important to highlight that the case of Beijing has not been considered in table 3 and for estimating the average values shown in tables AII.1 to AII.4. This location has been selected to show an extreme variation between the energy spectral losses of HCPV and PV devices, due to the high impact of aerosols on DNI and HCPV technology. However, this location should not be considered representative of the annual energy spectral losses of HCPV systems. As can be seen in table 3, the minimum difference is found with respect to the m-Si device with a maximum, minimum and average value of -6.14%, -2.45% and -4.3% respectively. The maximum difference is found with respect to the a-Si device with a maximum, minimum and average value of -10.56%, -4.38 and -6.2% respectively. As also shown, the minimum differences are always produced in Solar Village, while the maximum differences are produced in Granada (m-Si, p-Si and CIGS) and Alta Floresta (a-Si and CdTe). Finally, the annual average difference between all the HCPV and PV devices analysed at all sites considered has found to be about 5%.

HCPV*			
PV material	**Maximum (city)**	**Minimum (city)**	**Average**
m-Si	-6.14% (Granada)	-2.45% (Solar Village)	-4.26%
p-Si	-6.42% (Granada)	-2.66% (Solar Village)	-5.86%
a-Si	-10.56% (Alta Floresta)	-4.38% (Solar Village)	-6.25%
CdTe	-7.53% (Alta Floresta)	-2.83% (Solar Village)	-4.76%
CIGS	-6.35% (Granada)	-2.67% (Solar Village)	-4.29%
		Average	-5.09%

Table 3. Total maximum, minimum and average difference between the spectral impact of the HCPV and the PV technologies considered.
*Beijing has not been taken into account.

5. Conclusions

In this paper, the comparative assessment of the spectral impact on the energy yield at a monthly and annual time scale, of HCPV and PV technologies at several locations with disparate climate conditions has been conducted. In order to achieve this goal, several HCPV systems made up of different multi-junction solar cells and primary optics, and various single-junction commercial PV devices have been selected. The spectral impact of both technologies is evaluated thought the spectral factor index in conjunction with the Simple Model of Atmospheric Radiative Transfer of Sunshine (SMARTS). The comparison of both technologies is performed at five AERONET sites: Solar Village, Alta Floresta, Frenchman Flat, Granada and Beijing.

From the monthly analysis it can be concluded that, although the HCPV devices show a clear greater spectral dependence, both technologies show a seasonal behaviour. The higher and lower monthly variations for HCPV systems are found in Alta Floresta (-0.6 to -33.5% for the LM + PMMA) and Solar Village (-2.9% and -4.7% for the MM + SOG). With regard to the PV materials, the a-Si and CdTe show a similar and higher monthly spectral dependence than the others. The higher and lower monthly variations are found in Alta Floresta (8.6% to –5.6% for the a-Si) and Solar Village (-0.6% to -1.5% for the CdTe). The m-Si, p-Si and CIGS materials show a more stable performance with the higher and lower monthly spectral variations produced in Beijing (-0.5 to -3% for the p-Si) and Alta Floresta (0.1% to -0.3% for the p-Si) respectively. The analysis of the annual spectral impact on the energy yield also indicates that HCPV technology shows a higher spectral dependence. The lower annual spectral losses are produced in Alta Floresta (-3.9 to -5.2%), while the higher are produced at Beijing (-26.5% to -30.6%). Again, the a-Si and CdTe devices show the largest spectral dependence among all the PV materials. The best and worst performance of these devices are found in Alta Floresta (5.4%) and Beijing (-7.8%). The other PV materials show a more stable behaviour, the best and worst performances are found in Alta Floresta (-0.2%) and Beijing (-1.6%) respectively. Finally, it has been found that the current HCPV systems present annual spectral losses of around 5% with respect to PV systems at representative sites. This indicates that the spectral changes are not a crucial limitation for the market expansion of HCPV technology since their conversion efficiencies are significantly higher than PV technology.

Appendix I

As mentioned, the complete procedure followed in this paper is based on widely used techniques and mathematical expressions previously validated by the authors. Despite this, in this appendix the comparison between the simulated and actual data of two HCPV systems is conducted. In particular, the LM + PMMA and LM + SOG systems located at the Centro de Estudio Avanzados en Energía y Medio Ambiente (N 37º27’36’’, W 03º28’12’’) placed close to the Granada AERONET site, measured since January 2013, have been used. Figure AI.1 shows the experimental set-up to carry out the measurements, detailed information about this can be found in [6]. The spectral factor of the two HCPV systems is estimated from the short-circuit current (I_{sc}):

$$SF = \frac{\min(\int E_b(\lambda)\eta(\lambda)SR_i(\lambda)d\lambda) \int E_{b,ref}(\lambda)d\lambda}{min(\int E_{b,ref}(\lambda)\eta(\lambda)SR_i(\lambda)d\lambda) \int E_b(\lambda)d\lambda} = \frac{I_{sc}(25°C)}{I_{sc}^*}\frac{DNI^*}{DNI} \quad \text{(AI.1)}$$

as previously discussed in [53, 54], which is essentially the same magnitude as the one described by Sandia national Laboratories to spectrally correct the broadband irradiance [35]. Table A.I shows the simulated and actual impact of the spectral changes on the annual output of the two systems. As can be seen, the procedure followed in this work has a high accuracy with an annual difference lower than 1%.

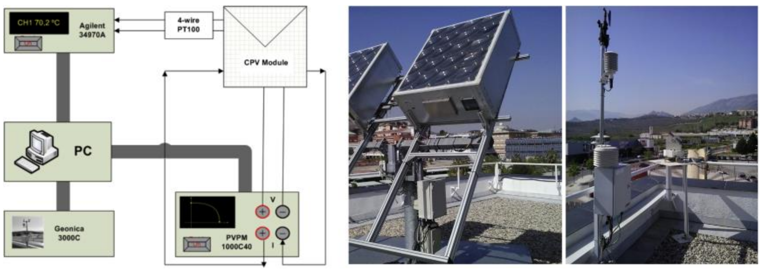

Figure AI.1. Experimental set-up to carry out this study at the roof top of the Centro de Estudios Avanzados en Energía y Medio Ambiente in southern Spain.

System	Simulated ΔE	Experimental ΔE
LM + PMMA	0.934	0.929
LM + SOG	0.949	0.941

Table AI.1. Simulated and experimental impact of the spectral variation on the annual energy yield of the two HCPV systems considered.

Appendix II

Tables AII.1 to AII.4 show the annual difference between the spectral impact of each HCPV system and the PV materials considered.

LM + PMMA*						
PV material	**Solar Village**	**Alta Floresta**	**Frenchman Flat**	**Granada**	**Beijing**	**Average**
m-Si	-5.17%	-3.91%	-5.52%	-6.14%	-29.90%	-5.18%
p-Si	-5.38%	-4.68%	-5.72%	-6.42%	-29.04%	-5.55%
a-Si	-7.10%	-10.25%	-7.53%	-8.62%	-22.84%	-8.37%
CdTe	-5.55%	-7.22%	-5.72%	-6.89%	-26.08%	-6.34%
CIGS	-5.39%	-4.06%	-5.79%	-6.35%	-29.73%	-5.40%

Table AII.1. Annual difference between the spectral impact of the HCPV LM + PMMA system and the PV materials considered.
*Beijing has not been taken into account in the estimation of the average values.

LM + SOG*						
PV material	**Solar Village**	**Alta Floresta**	**Frenchman Flat**	**Granada**	**Beijing**	**Average**
m-Si	-3.68%	-2.96%	-4.20%	-4.61%	-27.99%	-3.86%
p-Si	-3.89%	-3.74%	-4.40%	-4.90%	-27.13%	-4.23%
a-Si	-5.61%	-9.30%	-6.21%	-7.10%	-20.93%	-7.05%
CdTe	-4.05%	-6.27%	-4.40%	-5.36%	-24.17%	-5.02%
CIGS	-3.90%	-3.11%	-4.47%	-4.83%	-27.82%	-4.08%

Table AII.2. Annual difference between the spectral impact of the HCPV LM + SOG system and the PV materials considered.
*Beijing has not been taken into account in the estimation of the average values.

MM + PMMA*						
PV material	**Solar Village**	**Alta Floresta**	**Frenchman Flat**	**Granada**	**Beijing**	**Average**
m-Si	-3.81%	-4.22%	-4.13%	-4.83%	-27.83%	-4.25%
p-Si	-4.02%	-4.99%	-4.33%	-5.11%	-26.97%	-4.61%
a-Si	-5.74%	-10.56%	-6.13%	-7.31%	-20.77%	-7.44%
CdTe	-4.18%	-7.53%	-4.33%	-5.58%	-24.01%	-5.40%
CIGS	-4.03%	-4.37%	-4.40%	-5.04%	-27.66%	-4.46%

Table AII.3. Annual difference between the spectral impact of the HCPV MM + PMMA system and the PV materials considered.
*Beijing has not been taken into account in the estimation of the average values.

MM + SOG*						
PV material	**Solar Village**	**Alta Floresta**	**Frenchman Flat**	**Granada**	**Beijing**	**Average**
m-Si	-2.45%	-3.43%	-2.83%	-3.37%	-25.75%	-3.02%
p-Si	-2.66%	-4.21%	-3.03%	-3.65%	-24.90%	-3.39%
a-Si	-4.38%	-9.77%	-4.83%	-5.85%	-18.70%	-6.21%
CdTe	-2.83%	-6.75%	-3.03%	-4.11%	-21.93%	-4.18%
CIGS	-2.67%	-3.58%	-3.10%	-3.58%	-25.58%	-3.23%

Table AII.4. Annual difference between the spectral impact of the HCPV LM + SOG system and the PV materials considered.
*Beijing has not been taken into account in the estimation of the average values.

Acknowledgements

This work is supported by the Spanish Economy Ministry and the European Regional Development Fund / Fondo Europeo de Desarrollo Regional (ERDF / FEDER) under the project ENE2013-45242-R, by the Spanish Ministry of Education, Social Policy and Sports under the project ENE2009-08302 (FEDER Funds) and by the Andalusian Research Plan under the project P09-TEP-5045 (FEDER Funds). Eduardo F. Fernández is supported by the Spanish Ministry of Economy and Competitiveness through the Juan de la Cierva 2013 fellowship.

References

[1] A. Luque, G. Sala and I. Luque-Heredia, "Photovoltaic concentration at the onset of its commercial deployment," *Progress in Photovoltaics: Research and Applications,* vol. 14, no. 5, pp. 413-428, 2006.

[2] H. Cotal, C. Fetzer, J. Boisvert, G. Kinsey, R. King, P. Hebert, H. Yoon and N. Karam, "III-V multijunction solar cells for concentrating photovoltaics," *Energy and Environmental Science,* vol. 2, no. 2, pp. 174-192, 2009.

[3] S. P. Philipps, A. W. Bett, K. Horowitz and S. Kurtz, "Current status of concetrator photovotailc (CPV) technology," Fraunhofer ISE and NREL, 2015.

[4] Globaldata, "Globaldata. Concentrated Photovoltaics (CPV) – Global Market Size, Competitive Landscape and Key Country Analysis to 2020. 2014;UK.," 2014.

[5] D. Talavera, P. Pérez-Higueras, J. Ruíz-Arias and E. Fernández, "Levelised cost of electricity in high concentrated photovoltaic grid connected systems: Spatial analysis of Spain," *Applied Energy,* vol. 151, pp. 49-59, 2015.

[6] E. Fernández, P. Pérez-Higueras, A. Garcia Loureiro and P. Vidal, "Outdoor evaluation of concentrator photovoltaic systems modules from different manufacturers: First results and steps," *Progress in Photovoltaics: Research and Applications,* vol. 21, no. 4, pp. 693-701, 2013.

[7] P. Faine, S. Kurtz, C. Riordan and J. M. Olson, "The influence of spectral solar irradiance variations on the performance of selected single-junction and multi-junctions solar cells," *Solar Cells,* vol. 31, pp. 259 - 278, 1991.

[8] E. Fernández, G. Siefer, F. Almonacid, A. García-Loureiro and P. Pérez-Higueras, "A two subcell equivalent solar cell model for III–V triple junction solar cells under spectrum and temperature variations," *Solar Energy,* vol. 92, pp. 221-229, 2013.

[9] W. McMahon, K. Emery, D. Friedman, L. Ottoson, M. Young, J. Ward, C. Kramer, A. Duda and S. Kurtz, "Fill factor as a probe of current-matching for GaInP/GaAs tandem cells in a concentrator system during outdoor operation," *Progress in Photovoltaics: Research and Applications,* vol. 16, no. 3, pp. 213-224, 2008.

[10] M. Muller, B. Marion, S. Kurtz and J. Rodriguez, "An investigation into spectral parameters as they impact CPV module perfromance," *AIP conference proceedings,* vol. 1, pp. 307-311, 2010.

[11] J. Hashimoto, S. Kurtz, S. Keiichiro, M. Muller and K. Otani, "Performance of CPV sytem using three different types of III-V multi-junction solar cells," *AIP conference proceedings,* vol. 1477, pp. 372 -376, 2012.

[12] G. Peharz, G. Siefer and A. Bett, "A simple method for quatifying spectral impacts on multi-junction solar cells," *Solar Energy,* vol. 83, pp. 1588 - 1589, 2009.

[13] G. Peharz, J. Ferrer Rodríguez, G. Siefer and A. Bett, "A method for using CPV modules as temperature sensors and its application to rating procedures," *Solar Energy Materials and Solar Cells,* vol. 95, no. 10, pp. 2734-2744, 2011.

[14] B. García-Domingo, J. Aguilera, J. de la Casa and M. Fuentes, "Modelling the influence of atmospheric conditions on the outdoor real performance of a CPV (Concentrated Photovoltaic) module," *Energy,* vol. 70, pp. 239-250, 2014.

[15] H. A. Husna, "Impact of spectral irradiance distribution and temperature on the outdoor performance of concentrator photovoltaic system," *AIP Conference Proceedings,* vol. 1556, pp. 252-255, 2013.

[16] M. Victoria, S. Askins, R. Nuñez, Dominguez, R. Herrero, Antón., Sala.G. and J. Ruíz, "Tuning the current ration of a CPV system to maximiza the energy harvesting in a particular location," *AIP conference Proceedings,* vol. 1556, pp. 156-161, 2013.

[17] E. Fernández, F. Almonacid, J. Ruiz-Arias and A. Soria-Moya, "Analysis of the spectral variations on the performance of high concentrator photovoltaic modules operating under different real climate conditions," *Solar Energy Materials and Solar Cells,* Vols. 179-187, p. 127, 2014.

[18] A. Soria-Moya, E. F. Fernández, F. Almonacid and T. K. Mallick, "Spectral Losses of High Concentrator Photovoltaic Modules Depending on Latitude," *AIP conference proceedings,* 2015.

[19] N. Chan, H. Brindley and N. Ekins-Daukes, "Impact of individual atmospheric parameters on CPV system power, energy yield and cost of energy," *Progress in Photovoltaics: Research and Applications,* vol. 22, no. 10, p. 1080–1095, 2014.

[20] N. Chan, T. Young, H. Brindley, N. Ekins-Daukes, K. Araki, Y. Kemmoku and M. Yamaguchi, "Validation of energy prediction method for a concentrator photovoltaic module in Toyohashi Japan," *Progress in Photovoltaics: Research and Applications,* vol. 21, no. 8, pp. 1598-1610, 2013.

[21] T. Minemoto, M. Toda, S. Nagae, M. Gotoh, A. Nakajima, K. Yamamoto, H. Takakura and Y. Hamakawa, "Effect of spectral irradiance distribution on the outdoor performance of amorphous Si//thin-film crystalline Si stacked photovoltaic modules," *Solar Energy Materials and Solar Cells,* vol. 91, no. 2-3, pp. 120-122, 2007.

[22] T. Minemoto, S. Nagae and H. Takakura, "Impact of spectral irradiance distribution and temperature on the outdoor performance of amorphous Si photovoltaic modules," *Solar Energy Materials and Solar Cells,* vol. 91, no. 10, pp. 919-923, 2007.

[23] S. Nagae, M. Toda, T. Minemoto, H. Takakura and Y. Hamakawa, "Evaluation of the impact of solar spectrum and temperature variations on output power of silicon-based photovoltaic modules," *Solar Energy Materials and Solar Cells,* vol. 90, no. 20, pp. 3568-3575, 2006.

[24] Y. Nakada, S. Fukushige, T. Minemoto and H. Takakura, "Seasonal variation analysis of the outdoor performance of amorphous Si photovoltaic modules using the contour map," *Solar Energy Materials and Solar Cells,* vol. 93, no. 3, pp. 334-337, 2009.

[25] N. Katsumata, Y. Nakada, T. Minemoto and H. Takakura, "Estimation of irradiance and outdoor performance of photovoltaic modules by meteorological data," *Solar Energy Materials and Solar Cells,* vol. 95, no. 1, pp. 199-202, 2011.

[26] T. Ishii, K. Otani and T. Takashima, "Effects of solar spectrum and module temperature on outdoor performance of photovoltaic modules in round-robin measurements in Japan," *Progress in Photovoltaics: Research and Applications,* vol. 19, no. 2, pp. 141-148, 2011.

[27] G. Nofuentes, B. García-Domingo, J. V. Muñoz and F. Chenlo, "Analysis of the dependence of the spectral factor of some PV technologies on the solar spectrum distribution," *Applied Energy,* vol. 113, pp. 302-309, 2014.

[28] M. Alonso-Abella, F. Chenlo, G. Nofuentes and M. Torres-Ramírez, "Analysis of spectral effects on the energy yield of different PV (photovoltaic) technologies: The case of four specific sites," *Energy,* vol. 67, pp. 435-443, 2014.

[29] E. Fernandez, F. Cruz, T. Mallick and S. Sundaram, "Effect of Spectral Irradiance Variations on the Performance of Highly Efficient Environment-Friendly Solar Cells," *IEEE Journal of Photovoltaics,* vol. 5, no. 4, pp. 1150-1157, 2015.

[30] S. Senthilarasu, E. Fernández, F. Almonacid and T. Mallick, "Effects of spectral coupling on perovskite solar cells under diverse climatic conditions," *Solar Energy Materials and Solar Cells,* vol. 133, pp. 92-98, 2015.

[31] D. Dirnberger, G. Blackburn, B. Müller and C. Reise, "On the impact of solar spectral irradiance on the yield of different PV technologies," *Solar Energy Materials and Solar Cells,* vol. 132, pp. 431-442, 2015.

[32] J. Leloux, E. Lorenzo, B. García-Domingo, J. Aguilera and C. Gueymard, "A bankable method of assessing the performance of a CPV plant," *Applied Energy,* vol. 118, pp. 1-11, 2014.

[33] E. F. Fernandez, F. Almonacid, A. Soria-Moya and J. Terrados, "Experimental analysis of the spectral factor for quantifying the spectral influence on concentrator photovoltaic systems under real operating conditions," *Energy,* vol. 90, p. 1878–1886, 2015.

[34] E. Fernández, F. Almonacid, P. Rodrigo and P. Pérez-Higueras, "Calculation of the cell temperature of a high concentrator photovoltaic (HCPV) module: A study and comparison of different methods," *Solar Energy Materials and Solar Cells,* vol. 121, pp. 144-151, 2014.

[35] C. Osterwald, K. Emery and M. Muller, “Photovoltaic module calibration value versus optical air mass: The air mass function,” *Progress in Photovoltaics: Research and Applications,* vol. 22, no. 5, pp. 560-573, 2014.

[36] C. Monokroussos, M. Bliss, Y. Qiu, C. Hibberd, T. Betts, A. Tiwari and R. Gottschalg, “Effects of spectrum on the power rating of amorphous silicon photovoltaic devices,” *Progress in Photovoltaics: Research and Applications,* vol. 19, no. 6, pp. 640-648, 2011.

[37] C. Hibberd, F. Plyta, C. Monokroussos, M. Bliss, T. Betts and R. Gottschalg, “Voltage-dependent quantum efficiency measurements of amorphous silicon multi-junction mini-modules,” *Solar Energy Materials and Solar Cells,* vol. 95, no. 1, pp. 123-126, 2011.

[38] R. Núñez, C. Domínguez, S. Askins, M. Victoria, R. Herrero, I. Antón y G. Sala, «Determination of spectral variations by means of component cells useful for CPV rating and design,» *Progress in Photovoltaics: Research and Applications,* vol. in press, 2015.

[39] C. Rigollier, O. Bauer and L. Wald, “On the clear sky model of the ESRA - European Solar Radiation Atlas - With respect to the Heliosat method,” *Solar Energy,* vol. 68, no. 1, pp. 33-48, 2000.

[40] Y. A. Eltbaakh, M. Ruslan, M. Alghoul, M. Othman, K. Sopian and T. Razykov, “Solar attenuation by aerosols: An overview,” *Renewable and Sustainable Energy Reviews,* vol. 16, no. 6, pp. 4264-4276, 2012.

[41] C. Gueymard, “Impact of on-site atmospheric water vapor estimation methods on the accuracy of local solar irradiance predictions,” *Solar Energy,* vol. 101, pp. 74-82, 2014.

[42] C. Gueymard, “Parameterized transmittance model for direct beam and circumsolar spectral irradiance,” *Solar Energy,* vol. 71, no. 5, pp. 325-346, 2001.

[43] ASTM, “ASTM G 173-03 Standar tables for referecence solar spectral irradiance: direct normal and hemispherical on 37 tilted surface,” *American society for testing and materials,* pp. 1-20, 2012.

[44] J. Jaus and C. A. Gueymard, “Generalized spectral performance evaluation of multijunction solar cells using a multicore parallelized version of SMARTS,” *AIP confenrece proceedings,* vol. 1477, pp. 122 - 126, 2012.

[45] B. Holben, T. Eck, I. Slutsker, D. Tanré, J. Buis, A. Setzer, E. Vermote, J. Reagan, Y. Kaufman, T. Nakajima, F. Lavenu, I. Jankowiak and A. Smirnov, “AERONET - A federated instrument network and data archive for aerosol characterization,” *Remote Sensing of Environment,* vol. 66, no. 1, pp. 1-16, 1998.

[46] G. Camponogara, M. Silva Dias and G. Carrió, “Relationship between Amazon biomass burning aerosols and rainfall over the la Plata Basin,” *Atmospheric Chemistry and Physics,* vol. 14, no. 9, pp. 4397-4407, 2014.

[47] M. Chin, T. Diehl, O. Dubovik, T. Eck, B. Holben, A. Sinyuk and D. Streets, “Light absorption by pollution, dust, and biomass burning aerosols: A global model study and

evaluation with AERONET measurements," *Annales Geophysicae,* vol. 27, no. 9, pp. 3439-3464, 2009.

[48] I. Sabbah and F. Hasan, "Remote sensing of aerosols over the Solar Village, Saudi Arabia," *Atmospheric Research,* vol. 90, no. 2-4, pp. 170-179, 2008.

[49] A. Sayer, N. Hsu, C. Bettenhausen, M.-J. Jeong, B. Holben and J. Zhang, "Global and regional evaluation of over-land spectral aerosol optical depth retrievals from SeaWiFS," *Atmospheric Measurement Techniques,* vol. 5, no. 7, pp. 1761-1778, 2012.

[50] F. Kasten and A. T. Young, "Revised optical air mass tables and approximation formula," *Applied Optics,* vol. 28, no. 22, pp. 4735-4738, 1989.

[51] "Aerosol Robotic Network," 2015. [Online]. Available: http://aeronet.gsfc.nasa.gov/.

[52] E. F. Fernández, A. J. García-Loureiro y G. P. Smestad, «Multijunction concentrator solar cells: Analysis and fundamentals,» de *High Concentrator Photovoltaics: Fundamentals, Engineering and Power Plants, Pérez-Higueras, Pedro and Fernández, Eduardo F. (Eds.)*, Springer, 2015, pp. 9-37.

[53] E. Fernández and F. Almonacid, "Spectrally corrected direct normal irradiance based on artificial neural networks for high concentrator photovoltaic applications," *Energy,* vol. 74, no. C, pp. 941-949, 2014.

[54] F. Almonacid, E. Fernández, T. Mallick and P. Pérez-Higueras, "High concentrator photovoltaic module simulation by neuronal networks using spectrally corrected direct normal irradiance and cell temperature," *Energy,* vol. 84, pp. 336-343, 2015.

Figure Captions

Figure 1. Normalised spectral response of the lattice-matched and metamorphic-mismatched solar cells, and transmittance of the Fresnel lenses (PMMA and SOG) used for estimating the spectral factor.

Figure 2. Normalised spectral response of different single-junction photovoltaics materials used for estimating the spectral factor.

Figure 3. Impact on the global (denoted as G) and direct (denoted as D) spectral irradiance of air mass (top), aerosol optical depth at 550nm (middle) and precipitable water (bottom) simulated with the SMARTS model. The other parameters are kept constant at the reference values defined by the AM1.5d ASTMG-173-03 reference spectrum.

Figure 4. Individual impact of air mass on the performance of the HCPV (top) and PV (bottom) technologies under study. The other parameters are kept constant at the reference values defined by the AM1.5d ASTMG-173-03 reference spectrum.

Figure 5. Individual impact of aerosol optical depth on the performance of the HCPV (top) and PV (bottom) technologies under study. The other parameters are kept constant at the reference values defined by the AM1.5d ASTMG-173-03 reference spectrum.

Figure 6. Individual impact of aerosol optical depth on the performance of the HCPV (top) and PV (bottom) technologies under study. The other parameters are kept constant at the reference values defined by the AM1.5d ASTMG-173-03 reference spectrum.

Figure 7. Monthly-average values of aerosol optical depth at 550nm (AOD_{550}), Ångström exponent (α) and precipitable water (PW) obtained from AERONET for the five sites considered.

Figure 8. Impact of the spectral variation on the monthly energy yield of the HCPV materials under study for the five sites considered.

Figure 9. Impact of the spectral variation on the monthly energy yield of the PV materials under study for the five sites considered.

Figure 10. Impact of the spectral variation on the annual energy yield of the HCPV materials under study for the five sites considered.

Figure 11. Impact of the spectral variation on the annual energy yield of the PV materials under study for the five sites considered.

Figure AI.1. Experimental set-up to carry out this study at the roof top of the Centro de Estudios Avanzados en Energía y Medio Ambiente in southern Spain.